Functional and Morphological Development of Lymphoid Tissues and Immune Regulatory and Effector Function in Rhesus Monkeys: Cytokine-Secreting Cells, Immunoglobulin-Secreting Cells, and CD5+ B-1 Cells Appear Early in Fetal Development

Norbert Makori,[1,3] Alice F. Tarantal,[1] Fabien X. Lü,[1,3] Tracy Rourke,[1,3]
Marta L. Marthas,[1,2] Michael B. McChesney,[1]
Andrew G. Hendrickx,[1] and Christopher J. Miller[1,2,3]*

*California National Primate Research Center[1] and Department of Pathology, Microbiology and Immunology,[2]
School of Veterinary Medicine, and Center for Comparative Medicine,[3] University of California,
Davis, California 95616-8542*

Little is known regarding the timing of immune ontogeny and effector function in fetal humans and nonhuman primates. We studied the organization of lymphocyte and antigen-presenting cell populations in developing lymphoid tissues of rhesus monkey fetuses during the second and third trimesters (65 to 145 days of gestation; term = 165 days). Immunoglobulin-secreting and cytokine-secreting cells were detected at day 80. The thymus, spleen, lymph nodes, and intestinal mucosa were examined for cells expressing CD3, CD5, CD20, CD68, p55, and HLA-DR. In the spleens of 65-day-old fetuses (early second trimester), the overwhelming majority of total lymphocytes were CD5+ CD20+ B-1 cells. The remaining lymphocytes were CD3+ T cells. By day 80, splenic B and T cells were equal in number. Intraepithelial CD3+ CD5− T cells and lamina propria CD20+ CD5+ B cells were present in the intestines of 65-day-old fetuses. By day 80, numerous CD20+ CD5+ B cells were present in the jejunums and colons and early lymphocyte aggregate formation was evident. The spleens of 80- to 145-day-old fetuses contained immunoglobulin M (IgM)-secreting cells, while IgA-, IgG-, interleukin-6-, and gamma interferon-secreting cells were numerous in the spleens and colons. Thus, by the second trimester, the lymphoid tissues of the rhesus monkey fetus have a complete repertoire of properly organized antigen-presenting cells, T cells, and B cells.

Some aspects of the development of the human fetal lymphoid system and the emergence of phenotypically distinct lymphocyte subsets have been characterized (5, 17, 24, 34, 41, 48). However, those studies used small numbers of randomly collected, clinically derived specimens. Furthermore, the nature of these specimens has not permitted analysis of the development and location of cytokine-secreting cells and immunoglobulin (Ig)-secreting cells (ISCs) in normal human fetal lymphoid tissues. Although several studies with human neonates have shown that the immune system is fully developed at birth, the gestational age of emerging immune competence is not well described (1, 31, 36). The human fetal immune responses studied to date have been shown to be dominated by Th2 cytokines such as interleukin-4 (IL-4), IL-5, IL-6, IL-9, IL-10, and IL-13 (36).

Early in gestation, a population of B cells expressing CD5 characterizes fetal B-cell development. In both mice and humans, these CD5+ B cells are designated B-1a cells to distinguish them from a subset of CD5− B-1b cells with similar

attributes and from B-2 cells of bone marrow origin (22, 43, 51). The origins of CD5+ B cells in humans are believed to be the omentum, yolk sac, and fetal liver (51); however, the ultimate origin of CD5+ B-cell precursors is unclear. Greater than 90% of B cells in human fetal spleen, liver, and lymph nodes express CD5 throughout gestation (5, 7). B-1 cells produce low-affinity polyreactive Igs that have been termed natural antibodies (9, 15, 51). Fetal human and ovine B-1 cells express major histocompatibility complex (MHC) class II (17, 39), but fetal mouse B-1 cells do not (23). There is no published information on nonhuman primate fetal B-cell development or the normal ontogeny of lymphocyte subsets in the developing fetal rhesus monkey (*Macaca mulatta*) lymphoid system. In recent years it has become clear that additional information is needed on the developing rhesus monkey immune system due to the increased use of this species in biomedical research (13, 14, 44, 45). Rhesus monkeys and humans show similarities in their immune systems and responses (2, 3, 6, 25, 32, 40); therefore, rhesus monkeys are appropriate models for humans.

Present knowledge suggests that the newborn immune system is still developing compared with the level of development in the adult. However, the literature on this topic mainly deals with studies with rodents, but it is noteworthy that the newborn mouse is developmentally equivalent to a second-trimester hu-

* Corresponding author. Mailing address: California National Primate Research Center, University of California, Davis, One Shields Ave., Davis, CA 95616-8542. Phone: (530) 752-8584. Fax: (530) 754-4411. E-mail: cjmiller@ucdavis.edu.

TABLE 1. Timing of appearance of T cells, B cells, and APCs in spleen, axillary and mesenteric lymph nodes, jejunum and ileum, and colon of the fetal rhesus monkey

Fetal age (day)	Organ	Frequency of the following cell type[a]				
		CD3^{+} T cells	CD20^{+} CD5^{+} B cells	CD20^{+} CD5^{−} B cells	p55^{+} dendritic cells	CD68^{+} macrophages
65 ($n = 3$)	Spleen	1	3	0	1	3
	Axillary lymph node	0	0	0	1	1
	Mesenteric lymph node	1	1	0	1	1
	Jejunum and ileum	3	1	0	4	2
	Colon	ND	ND	ND	ND	ND
80 ($n = 7$)	Spleen[b]	3	3	0	2	2
	Axillary lymph node	2	3	0	3	3
	Mesenteric lymph node	2	2	0	1	1
	Jejunum and ileum	3	3	0	4	2
	Colon	2	2	0	4	1
100 ($n = 5$)	Spleen	4	3	1	3	2
	Axillary lymph node[b]	4	3	1	3	2
	Mesenteric lymph node[b]	2	2	1	2	2
	Jejunum and ileum[b]	4	3	3	4	3
	Colon**	3	3	1	4	2
145 ($n = 5$)	Spleen	4	4	1	2	2
	Axillary lymph node	4	4	2	4	3
	Mesenteric lymph node	4	4	2	4	3
	Jejunum and ileum	4	4	2	4	3
	Colon	4	4	2	4	3

[a] 0, not detected; 1, 1 to 2 cells/high-power field (×40 objective lens); 2, 5 to 10 cells/high-power field; 3, 10 to 50 cells/high-power field; 4, >50 cells/hpf high-power field; ND, not determined.
[b] By this stage of fetal development, compartmentalization into T- and B-cell areas was complete.

man fetus (29). Furthermore, mammalian species with short periods of gestation have less mature immune systems at birth than species with long gestational periods (10). In this regard, rhesus monkey gestation is 5 months, and the hallmarks of fetal development are very similar to those in the human (47).

In the present study, we characterized the lymphocyte and antigen-presenting cell (APC) populations in the developing lymphoid organs of fetal rhesus monkeys from the early second trimester (day 65 of gestation) to the late third trimester (day 145 of gestation). We found that CD20^{+} CD5^{+} B-1 cells expressing MHC class II molecules appear in large numbers early in the development of peripheral lymphoid organs and intestines. In contrast, CD3^{+} T cells were rare early in the second trimester but increased in number with advancing fetal age. The appearance of bone marrow-derived CD20^{+} CD5^{−} B-2 cells occurred later in gestation. Our findings indicate that lymphocyte subset differentiation occurs by the early second trimester, with lymphocytes present in nascent lymphoid tissues. Increasing lymphoid tissue organization into specific T- and B-cell areas in peripheral lymphoid organs was also evident later in the second trimester, a time when ISCs and cytokine-secreting cells were also present in these tissues.

MATERIALS AND METHODS

Fetal tissues. All animal procedures conformed to requirements of the Animal and Welfare Act, and the study protocols were approved prior to implementation by the Institutional Animal Use and Care Administrative Advisory Committee at the University of California, Davis. Normally cycling adult female rhesus monkeys ($n = 20$) were bred and identified as pregnant by ultrasound methods (46). Lymphoid organs (thymus, spleen, lymph nodes, intestines) were collected from 20 fetuses removed surgically by hysterotomy during the second (day 65 ± 2, $n = 3$; day 80 ± 3, $n = 7$; day 100 ± 2, $n = 5$) and third (day 145 ± 5, $n = 5$) trimesters. The gestation length in this species is 165 ± 10 days. Tissues from all fetuses were fixed in 10% buffered formalin, processed for embedment in paraffin, and then sectioned to a thickness of 5 to 6 μm. Representative sections from all organs were stained with hematoxylin-eosin for morphological assessment. A further 10 to 20 sections were analyzed after immunohistochemical and double immunofluorescent-antibody staining. Cell suspensions were prepared from fresh tissues of six of the fetuses for analysis by fluorescence-activated cell sorter FACS and enzyme-linked immunospot assay (ELISPOT).

Immunohistochemistry and immunofluorescence. The antibodies used included rabbit anti-human CD3 (polyclonal T cell; Dako, Carpinteria, Calif.) and mouse monoclonal anti-human clones of CD5 (clone CD5/54/F6; Dako), CD20 (clone L26; Dako), CD68 (clone KP1; Zymed, San Francisco, Calif.), HLA-DR (clone LN3; Zymed), and p55 (clone 55K-2; Dako). Fascin (p55) is an actin-binding protein that is commonly used as a marker for mature dendritic cells (DCs), in which it is abundantly expressed (28). Fascin is also expressed by some tumor cells (28). Isotype-matched IgG for the mouse monoclonal antibodies were used as negative controls and showed no reactivity. In order to enhance signal detection, all formalin-fixed tissue sections were subjected to antigen retrieval by immersion in AR 10 solution (Biogenex Corp., San Ramon, Calif.), followed by heating in a microwave oven on high power (500 to 1,000 W) for 3 min. Further heating was done at the 50% power level for an additional 10 min with the microwaves cycled on and off every 20 to 30 s. Immunohistochemistry with an avidin-biotin complex staining system was then performed. All washes between assay steps were done in phosphate-buffered saline (PBS; pH 7.4). Briefly, endogenous peroxidases were blocked by incubation with 1% hydrogen peroxide in PBS–0.5% Triton X-100 at room temperature for 20 min. To block nonspecific binding, sections were incubated with 10% normal goat serum, followed by application of the primary antibody for overnight incubation in a humidified chamber at 4°C. Biotinylated secondary antibodies were then applied for 30 min, and then horseradish peroxidase-streptavidin complex was applied for an additional 10 min. Immunoreactivity was visualized with 3,3′-diaminobenzidine, and the sections were counterstained with hematoxylin. Bright-field microscopy was used to analyze the stained tissue sections, and a subjective score of the frequency of cell types for each organ was noted (Table 1). Images of selected sections were digitized with National Institutes of Health Image soft-

CD20+ B cells   CD3+ T cells
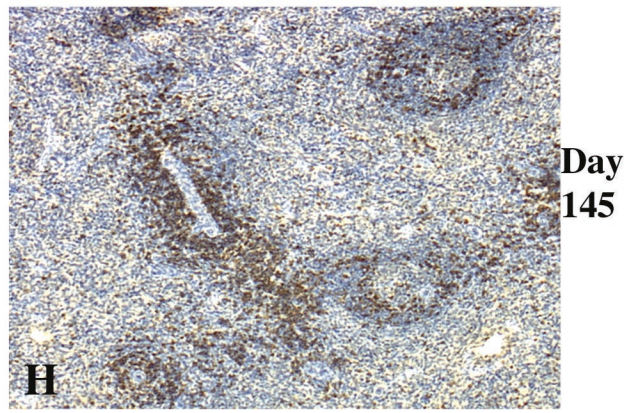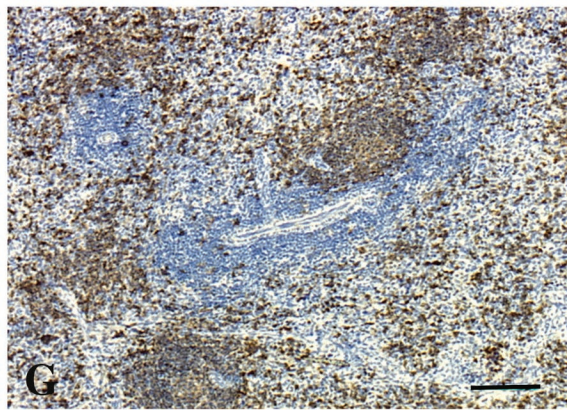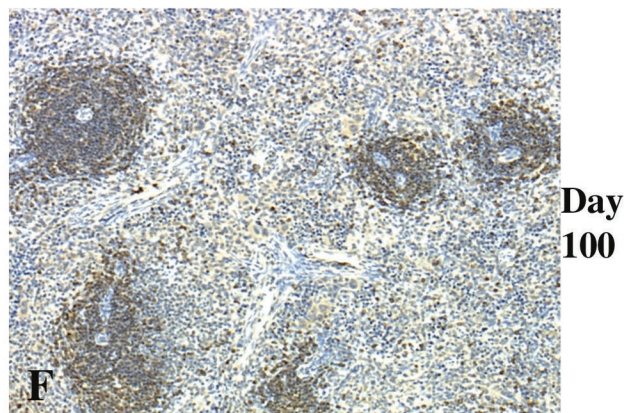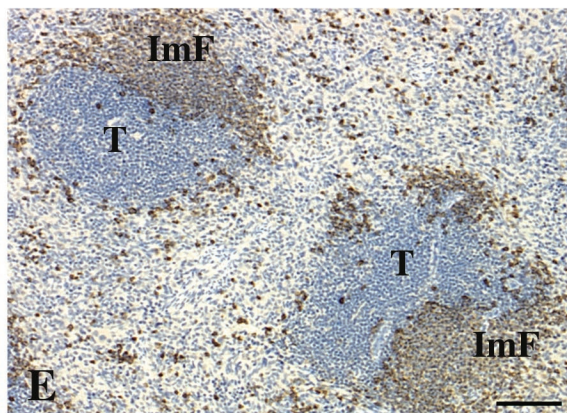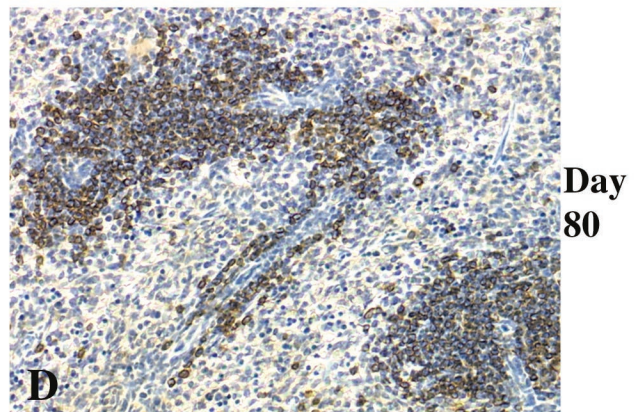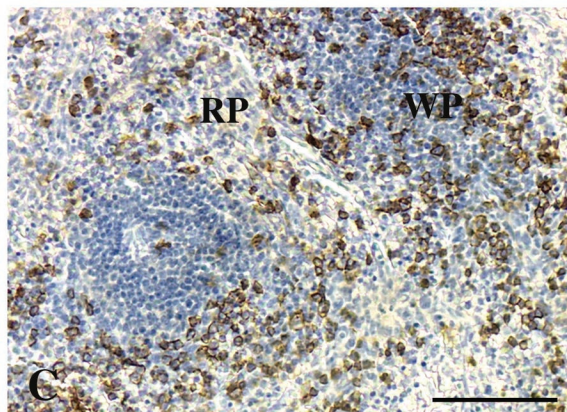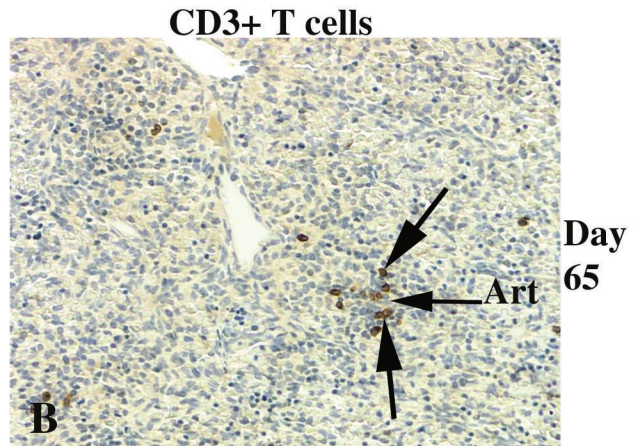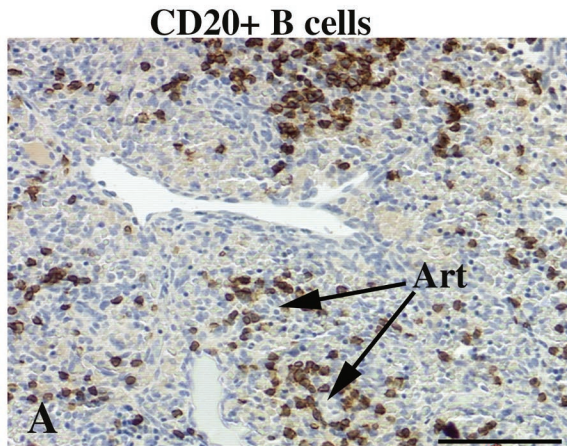
ware and Adobe PhotoShop (version 4.0) installed in a Macintosh computer (Apple Inc., Cupertino, Calif.).

For double immunofluorescence visualization, fluorescein isothiocyanate (FITC)- or Texas red-conjugated secondary antibodies (IgG) (Vector Laboratories, Inc., Burlingame, Calif.) were sequentially applied at a dilution of 1:50 after application of the respective primary antibodies. Since the monoclonal antibodies were of mouse origin (anti-CD20 with either anti-CD5 or anti-HLA-DR), a mouse-on-mouse blocking step was incorporated by using a commercial kit according to the instructions of the manufacturer (Vector Laboratories, Inc.). The slides were incubated in a humidified chamber for 1 h, washed four times with PBS, and mounted with Prolong antifade reagent (Molecular Probes, Leiden, Oreg.); and the fluorescence was observed and documented under UV irradiation on a Zeiss Axiophot microscope equipped with suitable filters. Images were captured as described above.

Flow cytometry. Cell suspensions were prepared from fresh fetal tissues processed in RPMI 1640 medium. A 50-μl aliquot from each sample was incubated for 20 min with 10 μl of each primary antibody. The samples were fixed, and the erythrocytes were lysed with the Coulter Q-Prep/ImmunoPrep system (Beckman Coulter, Fullerton, Calif.). The monoclonal antibodies used were conjugated with FITC (anti-CD3ε-SP34 and anti-HLA-DR-G46-6 [Pharmingen], anti-IgM [lot 039; Dako]), phycoerythrin (anti-CD4-M-T477; Pharmingen), allophycocyanin (anti-CD20-Leu16; Becton Dickinson, San Jose, Calif.), and peridinin chlorophyll-alpha protein (anti-CD8-Leu2a; Becton Dickinson). After the samples were stained, they were assessed on a fluorescence-activated cell sorter flow cytometry system (FACS Calibur; Becton Dickinson). For each measurement, a maximum of 10,000 gated lymphocyte events were collected. The data were analyzed with CellQuest software on a MacIntosh G4 computer (Apple Inc.).

Detection of cells spontaneously secreting Igs and cytokines. The frequency of ISCs was determined by the ELISPOT method (30). To detect IgG ISCs, 96-well nitrocellulose membrane plates (Millipore Corp., Bedford, Mass.) were coated with goat anti-monkey Ig (Fab plus Fc)/7s (Nordic Laboratories Inc., Capistrano, Calif.) at a concentration of 10 μg/ml in PBS (100 μl/well). To detect IgA ISCs, the plates were coated with rabbit anti-monkey IgA (Nordic Laboratories Inc.) diluted 1/1,000 in PBS (100 μl/well). To detect IgM ISCs, the plates were coated with rabbit anti-monkey IgM (Nordic Laboratories Inc.) diluted 1/2,000 in PBS (100 μl/well). The plates were then incubated overnight at 4°C in a humidified chamber with RPMI 1640 medium supplemented with 10% fetal calf serum (FCS). Diluted single-cell suspensions (from 10^6 to 10^4 cells in total) of the various lymphoid tissues were next incubated in the control plates at 37°C with 5% CO_2 for 16 h. The number of ISCs was determined by developing the plate with either a biotinylated goat anti-monkey IgG (Fc) (Nordic Laboratories Inc.) diluted 1/4,000 in 1% bovine serum albumin (BSA)-PBS or biotinylated goat anti-monkey IgA (Fc) (Nordic Laboratories Inc.) diluted 1/1,000 in 1% BSA-PBS or biotinylated goat anti-monkey IgM (Fc) (Nordic Laboratories Inc.) diluted 1/1,000 in 1% BSA-PBS, as appropriate. Avidin D-peroxidase (Vector Laboratories, Inc.) diluted 1/1,000 in 1% FCS-PBS was added to wells, followed by the addition of goat anti-avidin D-peroxidase (Vector Laboratories, Inc.) diluted 1/1,000 in 1% FCS-PBS. The plates were developed with the peroxidase substrate 3-amino-9-ethylcarbazole–H_2O_2 (Sigma) in acetate buffer (pH 5.0). Spots, which represented individual antibody-secreting cells, were counted with a stereomicroscope (Stemi 2000; Carl Zeiss, Munich, Hallbergmoos, Germany) under ×20 or ×40 magnification. The results were expressed as the number of ISCs per 10^6 mononuclear cells (MNCs). The numbers reported are the means for duplicate wells. Negative controls for each sample consisted of the cells added to wells that were not coated with the anti-monkey IgM, IgG, or IgA antibody. Additional controls included cell suspensions treated with cycloheximide (3.6×10^{-4} or 2×10^{-3} M; Sigma) during the incubation period. Treatment with cycloheximide inhibits Ig and cytokine spot formation by more than 95%.

RESULTS

**Lymphocyte populations and tissue distribution during fetal development. (i) Spleen.** The overwhelming majority of the lymphocytes within the spleens of the fetuses at 65 days of gestation (the earliest time point studied) were CD20$^+$ B cells (Table 1 and Fig. 1A). All of the CD20$^+$ cells also expressed CD5 and were randomly dispersed throughout the spleen, occasionally forming loose aggregates. Relatively few CD3$^+$ T cells were detected, and these were in small, loose clusters (Fig. 1B). Some B-cell clusters were associated with the ends of arterioles, consistent with initiation of lymphoid organization in the spleen. However, no distinct white pulp (WP) areas were observed in hematoxylin-eosin-stained sections of 65-day-old fetuses. In spleens collected from fetuses at day 80 of gestation, immature WP areas were distinct and populated by both CD20$^+$ CD5$^+$ B cells (Fig. 1C) and CD3$^+$ T cells (Fig. 1D). Most of the T cells were organized around arterioles in a layer two to three cells thick, whereas the B-cell layer was three to four cells thick. The immature B-cell follicles and the associated T-cell compartment of the developing WP were of similar size in most of the lymphoid aggregates at day 80. Between days 100 and 145, the splenic WP T-cell compartment increased more rapidly in size than did the B-cell follicle compartment (Fig. 1E to H). The developing splenic WP area expanded more rapidly than did the red pulp (RP) area. Thus, the ratio of the WP area to the RP area changed from 1:2 at day 80 to 1:1 by day 145. Since germinal centers are the hallmark of secondary lymphoid follicles, the lack of germinal centers in the developing splenic B-cell follicles at all stages studied suggests there was no antigen-driven clonal expansion of B cells or response within primary follicles.

(ii) Lymph nodes. The mesenteric lymph nodes of day-65-old fetuses were populated by a small number of CD3$^+$ T cells (Fig. 2A) and CD20$^+$ CD5$^+$ B cells (Fig. 2B) in a ratio of 1:1 (Table 1). In marked contrast to mesenteric lymph nodes, the axillary lymph node primordia at day 65 did not contain CD20$^+$ CD5$^+$ B cells or CD3$^+$ T cells but did have APCs (see below). By day 80, all lymph nodes had loose clusters of CD20$^+$ B and CD3$^+$ T cells with some evidence of organization into specific B-cell and T-cell compartments (Fig. 2C and D). The mesenteric lymph node had a higher level of organization than the axillary lymph node. By day 100, the B-cell and T-cell areas were more clearly defined (Fig. 2E and F), with the CD3$^+$ T-cell areas constituting the immature paracortex. The majority of the CD20$^+$ B cells were also CD5$^+$, but some CD20$^+$ CD5$^-$ cells were apparent, largely in the primitive follicles. The B cells formed a band at the outer margins of the cortex beneath the subcapsular sinus. In some areas, the B-cell band was thicker, consistent with early primary follicle formation. By day 145, the primary B-cell follicles in the outer cortex were clearly distinct (Fig. 2G), and more than 90% of the cells in the paracortical area stained intensely for CD3 (Fig. 2H).

FIG. 1. Spleens of fetal rhesus monkeys. At 65 days of gestation, >90% of the lymphocytes of the rhesus monkey fetus are B cells (A) with a few T cells (B). Note that some B-cell clusters and all T cells are associated with the ends of arterioles (Art). No distinguishable WP areas were apparent at day 65. (C and D) By day 80, immature WP areas (1:1 ratio of B to T cells) were distinct, with many B cells at the edge of the forming T-cell compartment. (E and F) Immature follicles (ImF in panel E) in the outer margins of the WP T-cell compartment (T) at day 100 of gestation. Note that at days 80 (D) and 100 (F), >80% of the T cells are in the WP, with the remainder scattered in the RP. The WP increased in size compared to the RP by day 145. (G) B cells; (H) T cells. Bars, 100 μm.
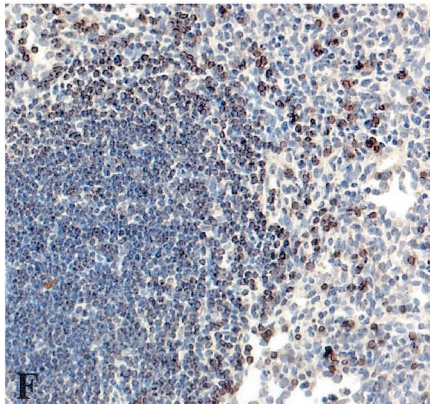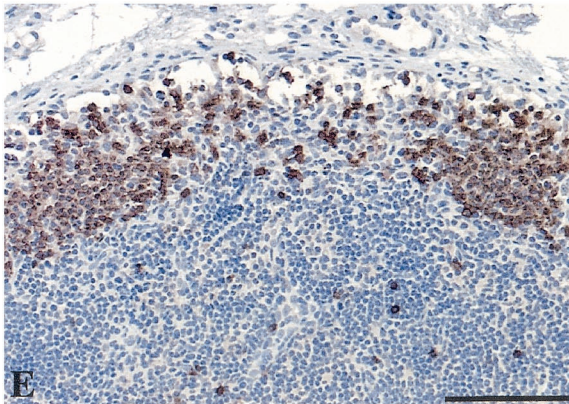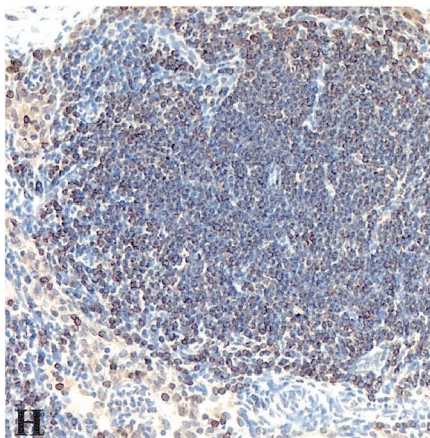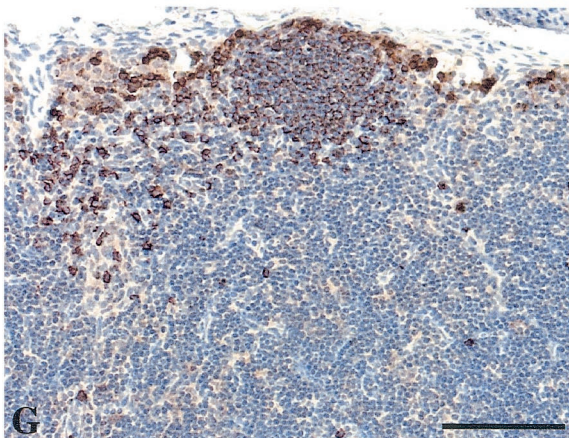
CD20+ B cells   CD3+ T cells
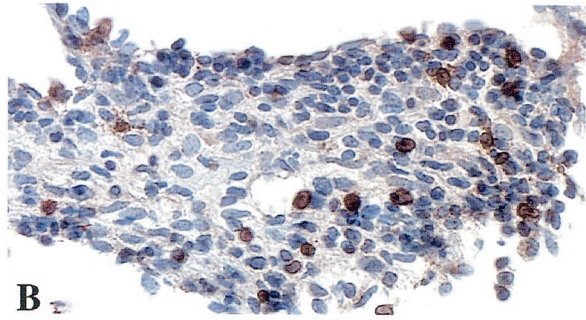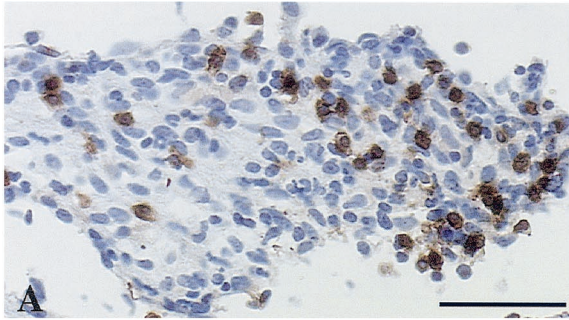
Day 65
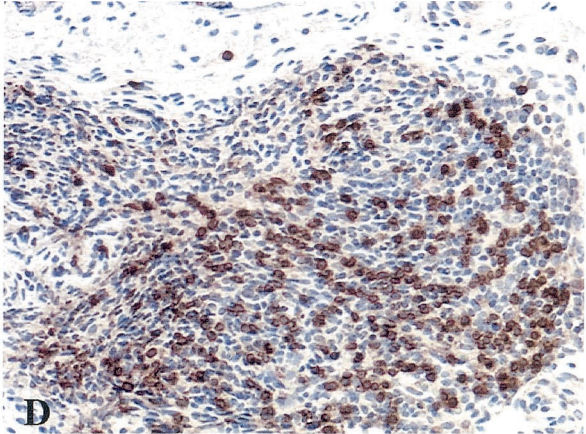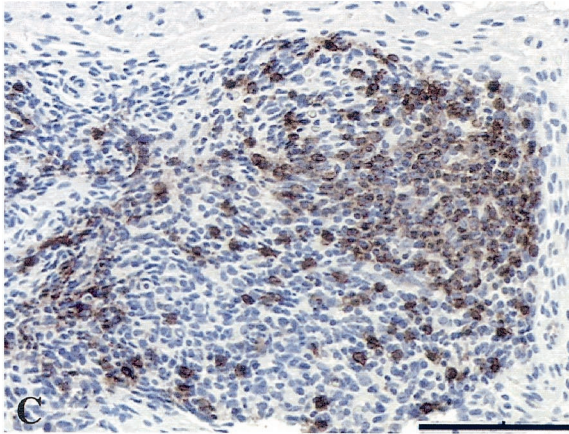
Day 80

Day 100

Day 145

(iii) **Intestine.** $CD3^+$ T cells and $CD20^+$ $CD5^+$ B cells were present in the lamina propria of the jejunum and ileum of fetuses at 65 days of gestation in a ratio of 1:1 (Table 1 and Fig. 3A). A few $CD3^+$ T cells were located in the intraepithelial compartment (Fig. 3B). Technical difficulties precluded analysis of the colon at day 65. By day 80, B-cell clusters and individual T cells were more frequent in the lamina propria of the jejunum, ileum, and colon (Fig. 3C and D). Between days 100 and 145, aggregates of T and B lymphocytes were formed in the lamina propria of the intestines (Table 1 and Fig. 3E to H). In these aggregates, the B cells were more numerous on the luminal side of the aggregates, while T cells were common on the muscularis side. Individual $CD3^+$ T cells were widely distributed in the intestinal lamina propria of older fetuses. The population of $CD3^+$ T cells was similar to that described in the gut of human fetuses at day 112 of gestation (early second trimester) (42).

(iv) **Thymus.** The thymic lobules of fetuses at day 65 of gestation were well developed, with a distinct medulla and cortex. The cortex had a greater lymphocyte density than the medulla. $CD20^+$ B cells were present at the corticomedullary junction (Fig. 4A), while most of the other thymocytes were immunoreactive to $CD3^+$ (Fig. 4B and D). In older fetuses there was an increase in the number of $CD20^+$ B cells within the medulla and at the corticomedullary junction (Fig. 4C), while the $CD3^+$ thymocyte frequency was similar in the medulla and cortex throughout gestation.

APC populations and tissue distribution. (i) Spleen. Numerous $CD68^+$ macrophages were scattered throughout the spleen in fetuses at 65 days of gestation (Table 1 and Fig. 5A), while p55-positive ($p55^+$) DCs were rare (Fig. 5B). Macrophages were less common in the WP areas at day 80, with most $CD68^+$ macrophages localized in the RP areas (Fig. 5C). By day 80, the ratio of macrophages to DCs (Fig. 5D) was 1:1, whereas it was ~10:1 in 65-day-old fetuses. By day 100, $p55^+$ DCs in the spleen were more common than macrophages, the ratio of macrophages (Fig. 5E) to DCs (Fig. 5F) being ~1:2. Most of the $p55^+$ DCs within the WP were localized in the T-cell compartment (Fig. 5F). At day 145, the distribution of the macrophages and DCs and the ratios of macrophages to DCs remained similar to those in 100-day-old fetuses. Thus, no differences were detected when fetuses in the late second trimester were compared to those in the middle to late third trimester.

(ii) **Lymph nodes.** At day 65, small populations of $CD68^+$ macrophages (Fig. 6A) and $p55^+$ DCs (Fig. 6B) were scattered in the developing mesenteric lymph nodes, whereas these cells were rare in the axillary lymph node primordia (data not shown). At day 80, $CD68^+$ macrophages (Fig. 6C) and $p55^+$ DCs (Fig. 6D) were increased in number and scattered throughout the parenchyma of the mesenteric and axillary lymph nodes. The ratio of macrophages to DCs at days 65 and 80 was 1:1 (Table 1). In older fetuses, most macrophages were localized in the medulla and outer cortical areas, whereas most DCs were associated with the developing T-cell area in the paracortex (Fig. 6E and F).

(iii) **Intestines.** At day 65, $CD68^+$ macrophages were sparsely scattered in the lamina propria (Fig. 7A) of the intestines, while $p55^+$ DCs were numerous and diffusely distributed within the lamina propria (Fig. 7B). The ratio of macrophages to DCs was ~1:10. In older fetuses, most macrophages were localized within developing lymphoid aggregates, with a few scattered in the lamina propria (Fig. 7C and E). The $p55^+$ DCs were also common in the lymphoid aggregates of older fetuses and had a morphology typical of DCs and showed more intense cytoplasmic staining (Fig. 7D and F) than the $p55^+$ DC-like cells diffusely distributed in the lamina propria. The significance of early colonization by $p55^+$ DCs is not clear.

Fetal $CD20^+$ B cells express CD5 and HLA-DR. To further evaluate the fetal B-cell phenotype and their potential roles as APCs during gestation, double immunofluorescence for analysis of CD20 and CD5 coexpression (Table 1) or CD20 and HLA-DR coexpression was done. Most of the B cells in the spleens, mesenteric lymph nodes (Fig. 8A to F), and small intestines of fetuses at days 65 and 80 of gestation expressed CD5. In the intestinal lymphoid aggregates, >95% of the B cells were $CD5^+$. $CD20^+$ $CD5^-$ B cells made up <1% of the B cells in all tissues of fetuses at days 65 to 100 of gestation. By day 145, the $CD20^+$ $CD5^-$ B cells were frequent in the developing B-cell follicles, even though most of the B cells in the lymphoid organs were still of the $CD20^+$ $CD5^+$ phenotype. The $CD20^+$ B cells in the thymic medulla weakly expressed CD5 at all fetal ages evaluated. In the thymuses, spleens, lymph nodes, and gut-associated lymphoid tissues of fetuses of all ages, 80 to 90% of the $CD20^+$ B cells were also HLA-DR positive. Thus, the B cells in all lymphoid tissues analyzed expressed MHC class II, suggesting that the development of antigen-presenting properties of the B cells occurs early during fetal ontogeny.

Spontaneous ISCs and cytokine-secreting cells in fetal lymphoid tissues. ISCs were present in the lymphoid tissues of fetuses at day 80 of gestation (the earliest gestation day analyzed). In the spleen and thymus, ISCs produced IgG, IgA, and IgM. Large numbers of IgG and IgA ISCs were found in the colon (Table 2). In five of six fetuses examined, the colon had the highest frequency of IgG ISCs. In four of these five fetuses, IgA ISCs also appeared in the colon at the highest frequency. The frequency of IgM ISCs in the thymus increased substantially between day 80 (17 to 19 cells per 10^6 MNCs) and day 100 (117 cells per 10^6 MNCs) of gestation, with fewer numbers of IgG and IgA spot-forming cells in the thymus at all fetal stages. At day 100, no IgG ISCs were detected in the spleen

FIG. 2. Mesenteric lymph nodes of fetal rhesus monkeys. At 65 days of gestation, a small number of B cells (A) and T cells (B) in a ratio of 1:1 were scattered among large numbers of mesenchymal cells. At 80 days of gestation, large numbers of B cells (C) and T cells (D) showed evidence of early organization into distinct T- and B-cell compartments. At day 100 of gestation, B cells (E) formed a thin layer outside the central T-cell area (F). At day 145 of gestation, B-cell follicles (G) were well defined, as was the T-cell compartment in the paracortex (H). The axillary lymph nodes had developmental features similar to those of the mesenteric lymph nodes, but axillary lymph node development was relatively delayed at day 65. Bars, 50 μm (A) and 100 μm (C, E, and G).

CD20+ B cells CD3+ T cells
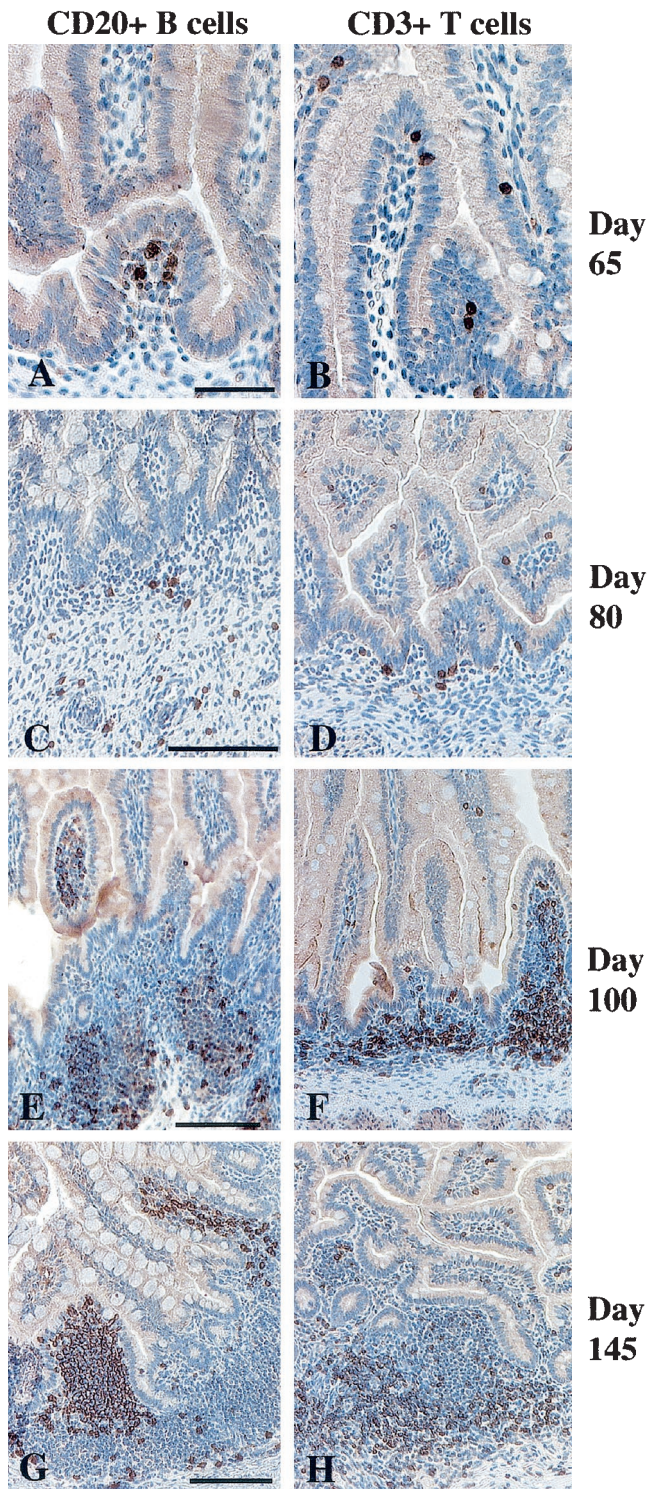

Day 65

Day 80

Day 100

Day 145

FIG. 3. Jejunums of fetal rhesus monkeys. At 65 days of gestation, B cells in the lamina propria (A) and scattered T cells mainly in the intraepithelial compartment (B); at 80 days of gestation, B-cell clusters (C) and individual T cells (D) in the lamina propria; (E to H) well-defined lymphoid aggregates in the lamina propria at day 100 (E and F) and day 145 (G and H) of gestation; (E and G) B cells on the luminal side of the aggregates; (F and H) widespread T cells in the lamina propria and concentrations of T cells on the muscularis side of the lymphoid aggregates. Bars, 50 μm (A) and 100 μm (C, E, and G).

and no IgA ISCs were detected in the colon due to technical difficulties with the cell isolation procedures. At day 145, IgG ISCs were detected in the spleen, axillary lymph nodes, and colon. At this later stage of gestation, there were IgM ISCs in the thymus, colon, and spleen and high numbers of IgA ISCs in the colon (Table 2). By comparison, the spleens of adult female rhesus monkeys have 4,000 to 16,000 IgG ISCs/10^6 MNCs and 100 to 500 IgA ISCs/10^6 MNCs, while the axillary lymph nodes of adult rhesus monkeys have 3,000 to 12,000 IgG ISCs/10^6 MNCs and 50 to 300 IgA ISCs/10^6 MNCs (30). Thus, fetal monkeys have far fewer ISCs than adult monkeys.

By day 100, IL-6-secreting cells were detected in the thymus, spleen, axillary lymph nodes, and colon (Table 3). A similar distribution was observed at day 145, except that no IL-6-secreting cells were detected in the colon. Gamma interferon (IFN-γ)-secreting cells were detected at day 80 in the thymus and colon. By day 100, the thymus, spleen, and colon had detectable IFN-γ-secreting cells. At day 145, there was an increase in IFN-γ-secreting cell frequency in the thymus, axillary lymph nodes, and colon, whereas the spleen had a lower frequency of IFN-γ-secreting cells compared to that at day 100. Of the tissues examined, the colon had the highest frequency of IFN-γ-secreting cells in three of four monkeys. Each of these three monkeys had detectable IL-6-secreting cells in at least some of the tissues analyzed. The increases in the frequencies of ISCs (B cells) and IFN-γ-secreting (T cells) in the colon at day 145 may have been due to local stimulation or selective accumulation of activated blasts.

Proportions of T- and B-cell subsets. Flow cytometric analysis of T- and B-cell populations was used to determine the frequency of T- and B-cell subsets in the fetal monkey thymus and spleen (Table 4). The frequency of the CD3$^+$ CD4$^+$ CD8$^+$ T-cell subset in the fetal thymus showed a modest decrease from day 80 (83 to 91%) to day 145 (70 to 73%). The frequency of this subset in the spleen was similar during the same time period (4% at day 80, 4 to 9% at day 145). CD20$^+$ B cells expressing IgM were present at a high frequency in the spleen at days 80 (7 to 15%), 100 (25 to 27%), and 145 (21 to 25%). ISCs were detected in all fetal spleens examined ($n = 6$) with the exception of one fetus that also had the lowest proportion (7%) of CD20$^+$ and IgM-positive B cells (Table 4), suggesting a direct relationship between ISC frequency and CD20$^+$ and IgM-positive B cells in the spleen. In comparison to the fetal monkey spleen (Table 4), the adult rhesus monkey spleen has 22 to 31% CD4$^+$ T cells, 24 to 42% CD8$^+$ cells, and 25 to 51% CD20$^+$ B cells, while the adult rhesus monkey axillary lymph node has 41 to 62% CD4$^+$ T cells, 14 to 34% CD8$^+$ T cells, and 12 to 34% B cells (37). Thus, fetal monkeys have far fewer T cells and approximately equal frequencies of B cells compared to those in adults.

DISCUSSION

On the basis of the results reported here, it is evident that there is considerable complexity in the lymphocyte populations of fetal rhesus monkeys by the early to middle of the second trimester (days 65 of 80 of gestation). In the secondary lymphoid organs (spleen, lymph nodes, and gut-associated lymphoid tissue), there was a more complex developmental sequence than in the thymus. ISCs and cytokine-secreting cells
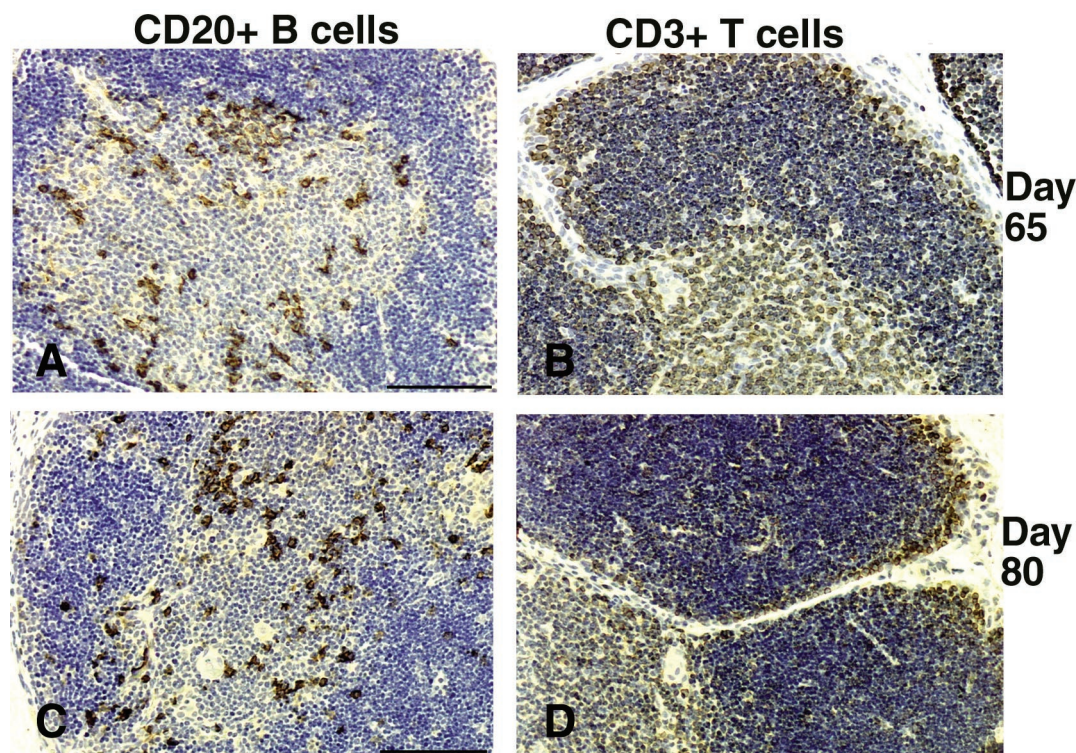
FIG. 4. Thymuses of fetal rhesus monkeys. (A and B) At day 65 of gestation, B cells can be seen throughout the corticomedullary junction (A) and intensely stained CD3$^+$ thymocytes can be seen in the cortex and medulla (B). (C and D) Similar cell populations were observed at day 80 and in older fetuses (data not shown). Bars, 100 μm.

were detected in lymphoid tissue at days 80 and 100 of gestation. The detection of ISCs correlated with the presence of large numbers of T cells and CD20$^+$ and IgM-positive B cells in lymphoid tissues and with the histologic organization in these organs. In older fetuses, the increase in B-cell number in the intestinal lamina propria correlated with the increased frequency of ISCs (IgG and IgA). Furthermore, the formation of immature B-cell follicles in the spleen at day 100 was associated with increases in the frequencies of IgA and IgM ISCs. The majority of B cells in all lymphoid tissues of the fetuses at days 80 and 100 of gestation were CD20$^+$ CD5$^+$ B-1 cells. In mouse and human fetuses, CD5$^+$ B-1 cells are also the first type of B cell found in intestinal and peripheral lymphoid tissues (5, 22). B-1 cells, which originate in the fetal omentum and liver (4, 35, 51), produce broadly reactive, low-affinity antibodies. These cells are self-replenishing during adult life, and the "natural" antibodies that they produce play a critical role in innate antimicrobial immunity (8, 16, 19, 22, 27). More CD20$^+$ CD5$^-$ B-2 cells were detected in the tissues of rhesus monkey fetuses at day 145 of gestation than in younger fetuses, but the CD5$^+$ B-1 cells remained the dominant B-cell phenotype. The increasing frequency of CD5$^-$ B-2 cells at later gestational ages is consistent with the gradual development of adaptive immunity (19). Although not determined in the present study, the origins of the B-1 cells in fetal rhesus monkeys are likely to be the fetal omentum and liver in humans (50) and in pigs and mice (16, 39).

Although we did not definitively determine the molecular signals associated with lymphoid development, the emergence of IFN-γ- and IL-6-producing cells in the spleen, colon, and axillary lymph nodes at day 100 was a clear indication of emerging immune effector function. In addition, the presence of IL-6-producing cells coincided with the definitive segregation of the T and B cells in the axillary lymph nodes into specific compartments. IL-6 is thought to be one of the regulators of T-cell development in murine lymph nodes (12), and our finding is consistent with this conclusion; thus, IL-6 appears to be a key mediator of organization in fetal rhesus monkey lymph nodes. The detection of IFN-γ-producing cells at day 100 in the peripheral lymphoid organs also coincided with the increased level of organization of the T-cell compartment. It has been reported that after T-cell-receptor-mediated stimulation, human neonatal T cells can produce IFN-γ and other cytokines at levels that are comparable to those produced by adult T cells (11). Thus, T cells in fetal lymphoid tissues are expressing critical immunoregulatory cytokines in the second trimester. These cytokines are likely involved in tissue organization but may also participate in adaptive immune responses.

In the spleen and mesenteric lymph nodes at day 80, the B cell:T cell ratio was ~1:1 and distinct T- and B-cell compartments were apparent. The peripheral lymph nodes and gut did not have well-defined T- and B-cell areas until day 100. Thus, T- and B-cell compartmentalization occurs first in the spleen and mesenteric lymph nodes and then in the peripheral lymph nodes and intestine.

Gene disruption experiments with mice have shown that the formation of distinct T- and B-cell compartments in mesenteric
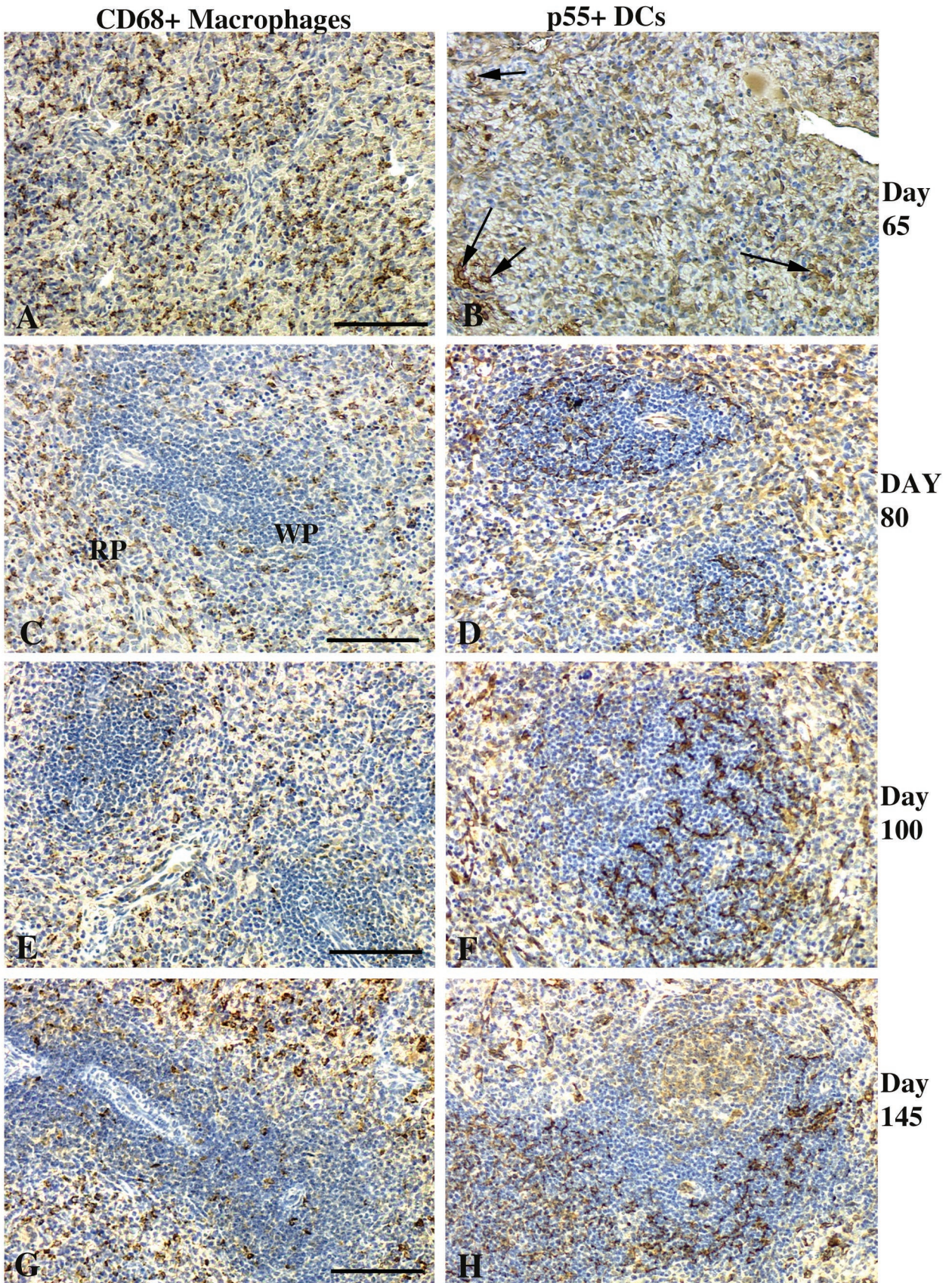
FIG. 5. Spleens of fetal rhesus monkeys. At day 65 of gestation, CD68$^+$ macrophages (A) and p55$^+$ DCs (arrows) (B); at day 80 of gestation (C and D) and day 100 of gestation (E and F), macrophages in the RP with a few scattered in the WP (C and E); (D and F) DCs located within the WP T-cell areas; (G) at day 145 of gestation, macrophages common in the WP; (H) DCs mainly in T-cell areas. Bars, 100 μm.

CD68+ Macrophages   **p55+ DCs**
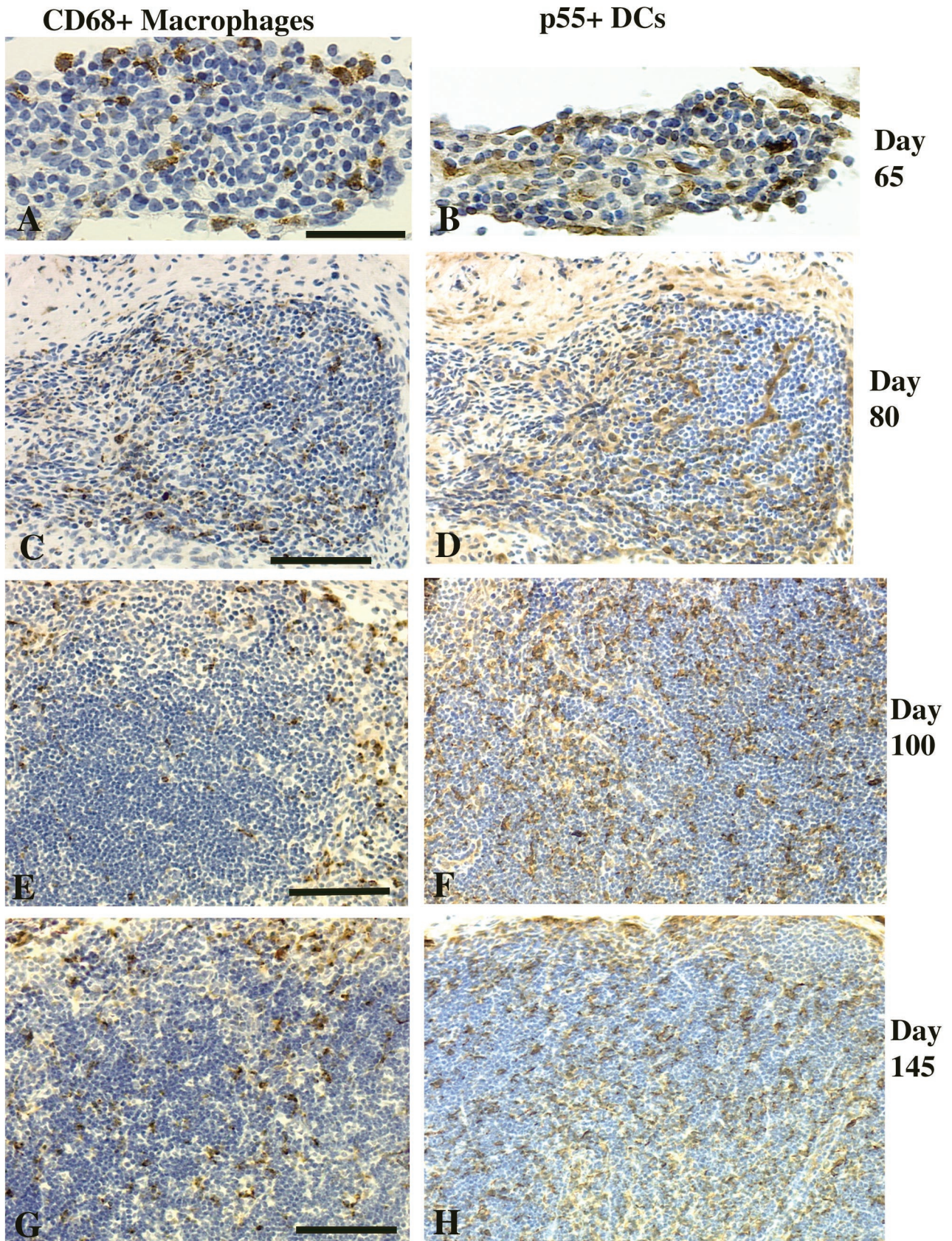
FIG. 6. Mesenteric lymph nodes of fetal rhesus monkeys. At day 65 of gestation, scattered macrophages (A) and a few DCs (B) can be seen. At day 80 of gestation, the macrophage (C) and DC (D) populations had increased. At day 100 (E) and day 145 (G) of gestation, macrophages were concentrated in the outer cortex, while at day 100 (F) and day 145 (H) of gestation, the DCs were mainly confined to the paracortex. Bars, 50 μm (A) and 100 μm (C, E, and G).

CD68+ Macrophages   **p55+ DCs**

Day 65

Day 100

Day 145
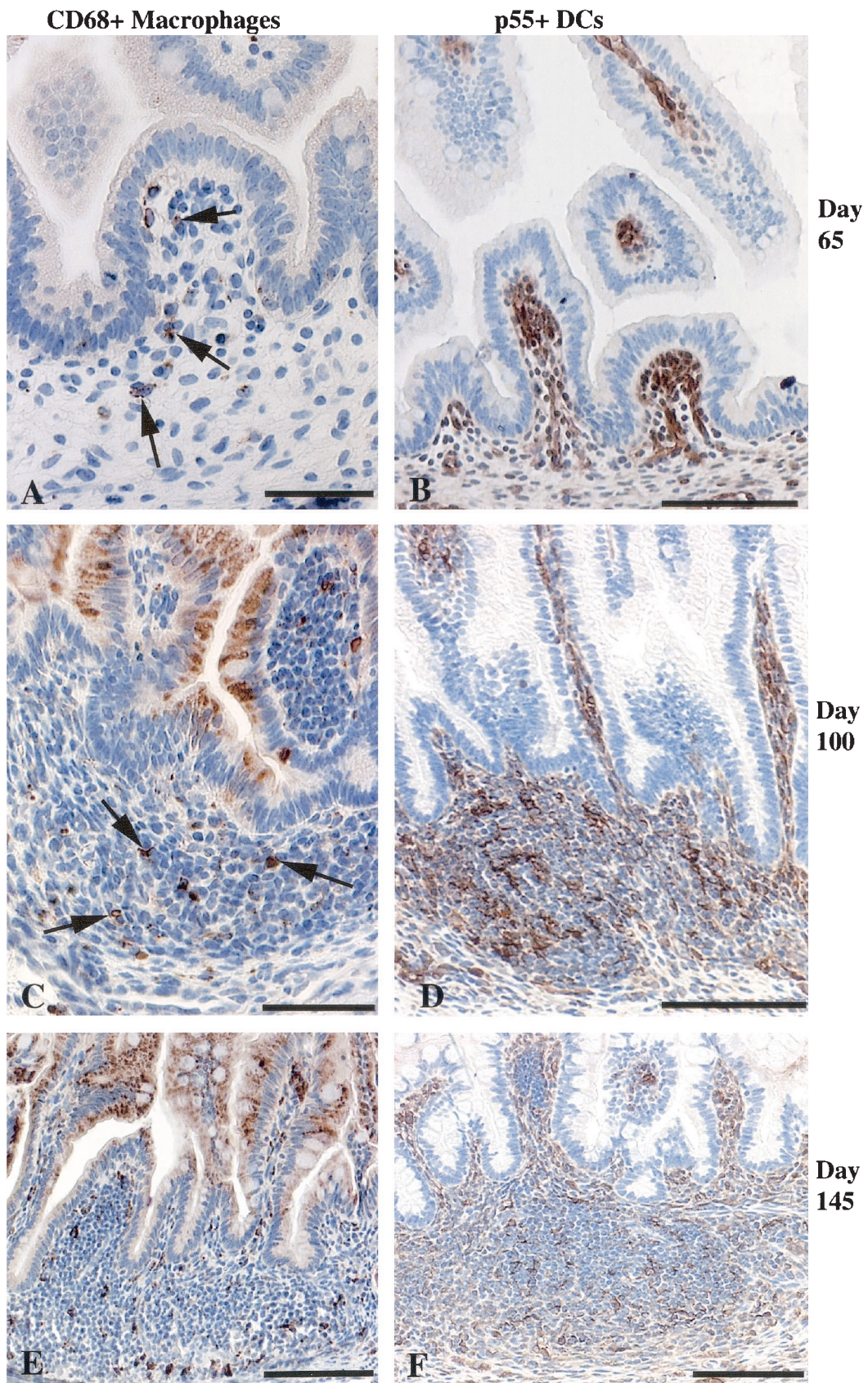
FIG. 7. Jejunums, ileums, and colons of fetal rhesus monkeys. (A and B) At day 65 of gestation, macrophages were few (A; arrows), while p55[+] DCs were numerous (B) throughout the gut lamina propria, especially at the tips of villi. (C and D) In lymphoid aggregates at day 100 of gestation, macrophages were rare in the T-cell areas (C; arrows), while DCs were numerous (D). (E) At day 145 of gestation, macrophages were numerous within the lymphoid aggregates. (F) DCs were located in T-cell areas. Bars, 50 μm (A and C) and 100 μm (B to F).

CD20+ B cells   CD5+ cells   CD20+CD5+

FIG. 8. Fetal CD20$^+$ B cells express CD5. Double immunofluorescence with anti-CD20 (A and D; Texas red) and anti-CD5 (B and E; FITC green) in the spleen (A, B, and C) and mesenteric lymph nodes (D, E, and F) at day 65 of gestation shows double-stained cells. The majority of the CD20$^+$ B cells in all lymphoid tissues at days 65 to 145 of gestation expressed CD5. Double-labeled cells are yellow, CD5$^+$ single-labeled positive cells are green, and CD20$^+$ single-labeled positive cells are red. Magnification, ×340.

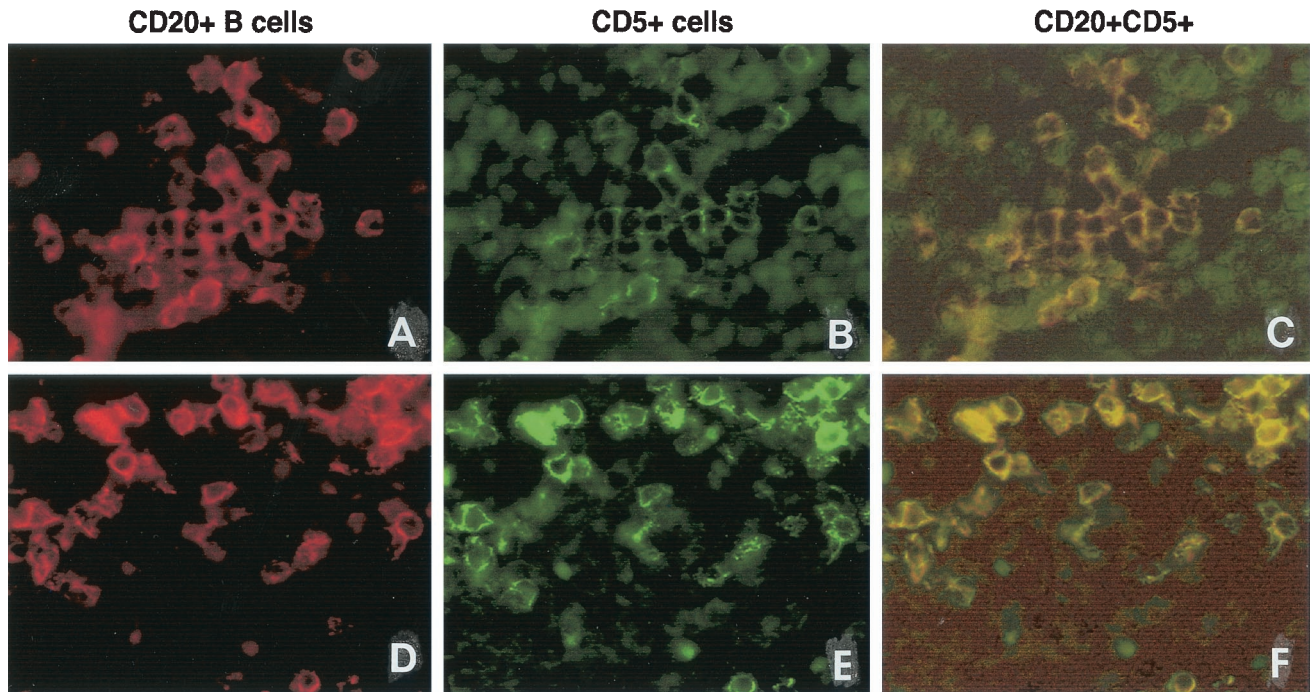lymph nodes requires expression of tumor necrosis factor receptor I, whereas in the spleen, lymphotoxin-α has been identified as the main signal (18, 20) that regulates B- and T-cell zone formation. Such differences in signal requirements for segregation of T and B cells into specific zones may be one of the factors influencing the differential timing of development of T- and B-cell compartments in the lymph nodes and spleen and possibly other lymphoid tissues. Definitive segregation of lymphocytes into T- and B-cell compartments in peripheral lymph nodes by day 100 also coincided with the specific localization of p55$^+$ DCs in the T-cell compartments.

In the developing rhesus monkey thymus, CD20$^+$ B cells were observed at day 65, and these cells increased in numbers in the thymuses of older fetuses. Thymic B cells act primarily as APCs in the negative selection of thymocytes and may not necessarily play a role as antibody-producing cells (21). It has been proposed that both thymic DCs and B cells play a major role in inducing neonatal tolerance to major self-antigens (26, 33, 38). IFN-γ-presenting cells were also more frequent in the thymuses of older fetuses and coincided with a decrease in the

TABLE 2. Frequency^a of spontaneous ISCs in thymus, spleen, and colon of the fetal rhesus monkey

Fetal age (days) and fetus no.	Frequency of ISCs (no. of ISCs/10⁶ MNCs) in:											
	Thymus			Spleen			Axillary lymph node			Colon		
	IgG	IgA	IgM	IgG	IgA	IgM	IgG	IgA	IgM	IgG	IgA	IgM
80												
1	0	6	17	0	0	0	0	0	0	1150	5,500	0
2	11	0	19	106	266	851	0	0	0	11,765	10,000	0
100												
3	0	43	117	0	269	1,923	0	0	0	0	0	0
4	0	5	8	0	71	316	0	0	0	5,426	0	0
145												
5	0	5	59	14	16	295	607	0	0	38,181	3,750	429
6	0	2	29	13	1	139	10	0	8	34,375	88	250

^{a} The frequency of (ISCs) was measured by the ELISPOT method (see Materials and Methods).

TABLE 3. Frequency^a of spontaneous cytokine-secreting cells in thymus, spleen, lymph node, and colon cells of the fetal rhesus monkey

Fetal age (days) and fetus no.	Frequency of cytokine-secreting cells (no. of cells/10⁶ MNCs) in:							
	Thymus		Spleen		Axillary lymph node		Colon	
	IL-6	IFN-γ	IL-6	IFN-γ	IL-6	IFN-γ	IL-6	IFN-γ
80								
1	ND^b	ND	ND	ND	ND	ND	ND	ND
2	0	31	0	0	0	0	0	1,470
100								
3	ND	ND	ND	ND	ND	ND	ND	ND
4	100	3	1,150	1,000	15,789	0	319	1,489
145								
5	197	4	3,909	626	0	0	0	13,961
6	27	18	3,597	1,111	227	316	0	71,875

^{a} The frequency of cytokine-secreting cells was measured by the ELISPOT method.
^{b} ND, not determined.

TABLE 4. Frequency of lymphocyte subsets in the fetal rhesus monkey thymus and spleen as determined by flow cytometry

Subset	Frequency (%) at:											
	Day 80				Day 100				Day 145			
	Thymus		Spleen		Thymus		Spleen		Thymus		Spleen	
	Fetus 1	Fetus 2	Fetus 1	Fetus 2	Fetus 3	Fetus 4	Fetus 3	Fetus 4	Fetus 5	Fetus 6	Fetus 5	Fetus 6
CD3$^+$ CD4$^+$	6.5	4.0	20.5	20.9	20.1	7.0	11.4	28.1	9.8	12.3	54.3	66.0
CD3$^+$ CD8$^+$	5.0	4.4	9.9	8.3	20.0	7.3	13.5	9.6	10.1	12.0	28.3	12.2
CD3$^+$ CD4$^+$ CD8$^+$	82.5	90.9	5.1	4.2	56.4	84.3	5.7	4.2	73.3	70.2	9.1	4.3
CD20$^+$ IgM positive	ND^a	ND	7.3	14.9	ND	ND	26.6	25.1	ND	ND	24.5	20.8

^{a} ND, not determined.

frequency of CD3$^+$ CD4$^+$ CD8$^+$ T cells in older fetuses (Table 4).

This study demonstrates that, by the second trimester, the rhesus monkey fetus has a complete complement of immune cells that are properly positioned within the developing lymphoid organ compartments to perform their respective roles in adaptive immune responses. In addition, the lymphoid tissues of the fetal rhesus monkey contain ISCs and cytokine-secreting cells, suggesting that the fetal rhesus monkey has a well-developed immune system with the potential to generate immune responses. This conclusion is consistent with those of studies that have shown that infants are capable of responding to many test antigens or vaccines in a manner similar to that in adults (50) and studies with fetal baboons (49) and rhesus monkeys (K. M. Lockridge, A. F. Tarantal, S. Salamat, W. J. Brian, S. S. Zhou, and P. A. Barry, submitted for publication) in which specific antibody responses have been shown after direct in utero immunization. Taken together, it is apparent that the fetal primate, to some degree, develops immune effector function during gestation. However, the potential of this fetal immunologic immune system to mount antigen-specific immune responses requires further study in order to better understand the role of perinatal immunization strategies to prevent infectious diseases in neonates.

REFERENCES

1. **Ahluwalia, B., B. Wesley, O. Adeyiga, D. M. Smith, A. Da-Silva, and S. Rajguru.** 2000. Alcohol modulates cytokine secretion and synthesis in human fetus: an in vivo and in vitro study. Alcohol **21:**207–213.
2. **Attanasio, R., J. S. Allan, S. A. Anderson, T. C. Chanh, and R. C. Kennedy.** 1991. Anti-idiotypic antibody response to monoclonal anti-CD4 preparations in nonhuman primate species. J. Immunol. **146:**507–514.
3. **Bals, R., C. Lang, D. J. Weiner, C. Vogelmeier, U. Welsch, and J. M. Wilson.** 2001. Rhesus monkey (*Macaca mulatta*) mucosal antimicrobial peptides are close homologues of human molecules. Clin. Diagn. Lab. Immunol. **8:**370–375.
4. **Baumgarth, N., O. C. Herman, G. C. Jager, L. Brown, and L. A. Herzenberg.** 1999. Innate and acquired humoral immunities to influenza virus are mediated by distinct arms of the immune system. Proc. Natl. Acad. Sci. USA **96:**2250–2255.
5. **Bhat, N. M., A. B. Kantor, M. M. Bieber, A. M. Stall, L. A. Herzenberg, and N. N. Teng.** 1992. The ontogeny and functional characteristics of human B-1 (CD5$^+$ B) cells. Int. Immunol. **4:**243–252.
6. **Black, C. M., J. S. McDougal, R. C. Holman, B. L. Evatt, and C. B. Reimer.** 1993. Cross-reactivity of 75 monoclonal antibodies to human immunoglobulin with sera of non-human primates. Immunol. Lett. **37:**207–213.
7. **Bofill, M., G. Janossy, M. Janossa, G. D. Burford, G. J. Seymour, P. Wernet, and E. Kelemen.** 1985. Human B cell development. II. Subpopulations in the human fetus. J. Immunol. **134:**1531–1538.
8. **Carroll, M. C., and A. P. Prodeus.** 1998. Linkages of innate and adaptive immunity. Curr. Opin. Immunol. **10:**36–40.
9. **Casali, P., S. E. Burastero, M. Nakamura, G. Inghirami, and A. L. Notkins.** 1987. Human lymphocytes making rheumatoid factor and antibody to ssDNA belong to Leu-1$^+$ B-cell subset. Science **236:**77–81.
10. **Chappuis, G.** 1998. Neonatal immunity and immunisation in early age: lessons from veterinary medicine. Vaccine **16:**1468–1472.
11. **Chipeta, J., Y. Komada, X. L. Zhang, E. Azuma, H. Yamamoto, and M. Sakurai.** 2000. Neonatal (cord blood) T cells can competently raise type 1 and 2 immune responses upon polyclonal activation. Cell. Immunol. **205:**110–119.
12. **Clegg, C. H., H. S. Haugen, J. T. Rulffes, S. L. Friend, and A. G. Farr.** 1999. Oncostatin M transforms lymphoid tissue function in transgenic mice by stimulating lymph node T-cell development and thymus autoantibody production. Exp. Hematol. **27:**712–725.
13. **Coe, C. L., and G. R. Lubach.** 2000. Prenatal influences on neuroimmune set points in infancy. Ann. N. Y. Acad. Sci. **917:**468–477.
14. **Cowan, M. J., S. H. Chou, and A. F. Tarantal.** 2001. Tolerance induction post in utero stem cell transplantation. Ernst Schering Res. Found. Workshop **33:**145–171.
15. **Cramer, D. V.** 2000. Natural antibodies and the host immune responses to xenografts. Xenotransplantation **7:**83–92.
16. **Cukrowska, B., J. Sinkora, Z. Rehakova, M. Sinkora, I. Splichal, L. Tuckova, S. Avrameas, A. Saalmuller, R. Barot-Ciorbaru, and H. Tlaskalova-Hogenova.** 1996. Isotype and antibody specificity of spontaneously formed immunoglobulins in pig fetuses and germ-free piglets: production by CD5$^-$ B cells. Immunology **88:**611–617.
17. **Edwards, J. A., B. M. Durant, D. B. Jones, P. R. Evans, and J. L. Smith.** 1986. Differential expression of HLA class II antigens in fetal human spleen: relationship of HLA-DP, DQ, and DR to immunoglobulin expression. J. Immunol. **137:**490–497.
18. **Ettinger, R., J. L. Browning, S. A. Michie, W. van Ewijk, and H. O. McDevitt.** 1996. Disrupted splenic architecture, but normal lymph node development in mice expressing a soluble lymphotoxin-beta receptor-IgG1 fusion protein. Proc. Natl. Acad. Sci. USA **93:**13102–13107.
19. **Fearon, D. T., and R. M. Locksley.** 1996. The instructive role of innate immunity in the acquired immune response. Science **272:**50–53.
20. **Fu, Y. X., G. Huang, M. Matsumoto, H. Molina, and D. D. Chaplin.** 1997. Independent signals regulate development of primary and secondary follicle structure in spleen and mesenteric lymph node. Proc. Natl. Acad. Sci. USA **94:**5739–5743.
21. **Fukuba, Y., M. Inaba, S. Taketani, Y. Hitoshi, Y. Adachi, R. Tokunaga, K. Inaba, K. Takatsu, and S. Ikehara.** 1994. Functional analysis of thymic B cells. Immunobiology **190:**150–163.
22. **Hayakawa, K., and R. R. Hardy.** 2000. Development and function of B-1 cells. Curr. Opin. Immunol. **12:**346–353.
23. **Hayakawa, K., D. Tarlinton, and R. R. Hardy.** 1994. Absence of MHC class II expression distinguishes fetal from adult B lymphopoiesis in mice. J. Immunol. **152:**4801–4807.
24. **Hayward, A. R.** 1981. Development of lymphocyte responses and interactions in the human fetus and newborn. Immunol. Rev. **57:**39–60.
25. **Helmuth, E. F., N. L. Letvin, and D. H. Margolin.** 2000. Germline repertoire of the immunoglobulin V(H)3 family in rhesus monkeys. Immunogenetics **51:**519–527.
26. **Inaba, M., K. Inaba, M. Hosono, T. Kumamoto, T. Ishida, S. Muramatsu, T. Masuda, and S. Ikehara.** 1991. Distinct mechanisms of neonatal tolerance induced by dendritic cells and thymic B cells. J. Exp. Med. **173:**549–559.
27. **Kasaian, M. T., and P. Casali.** 1993. Autoimmunity-prone B-1 (CD5 B) cells, natural antibodies and self recognition. Autoimmunity **15:**315–329.
28. **Kureishy, N., V. Sapountzi, S. Prag, N. Anilkumar, and J. C. Adams.** 2002. Fascins, and their roles in cell structure and function. Bioessays 24:350–361.
29. **Lawton, A., and M. Cooper.** 1996. Ontogeny of immunity, p. 1–13. *In* E. Stiehm (ed.), Immunologic disorders in infants and children, 4th ed. The W. B. Saunders Co., Philadelphia, Pa.

30. **Lu, F. X., K. Abel, Z. Ma, T. Rourke, D. Lu, J. Torten, M. McChesney, and C. J. Miller.** 2002. The strength of B cell immunity in female rhesus macaques is controlled by CD8^{+} T cells under the influence of ovarian steroid hormones. Clin. Exp. Immunol. **128:**10–20.

31. **Malhotra, I., J. Ouma, A. Wamachi, J. Kioko, P. Mungai, A. Omollo, L. Elson, D. Koech, J. W. Kazura, and C. L. King.** 1997. In utero exposure to helminth and mycobacterial antigens generates cytokine responses similar to that observed in adults. J. Clin. Investig. **99:**1759–1766.

32. **Martin, L. N.** 1982. Chromatographic fractionation of rhesus monkey (Macaca mulatta) IgG subclasses using DEAE cellulose and protein A-sepharose. J. Immunol. Methods **50:**319–329.

33. **Mazda, O., Y. Watanabe, J. Gyotoku, and Y. Katsura.** 1991. Requirement of dendritic cells and B cells in the clonal deletion of MLS-reactive T cells in the thymus. J. Exp. Med. **173:**539–547.

34. **Namikawa, R., T. Mizuno, H. Matsuoka, H. Fukami, R. Ueda, G. Itoh, M. Matsuyama, and T. Takahashi.** 1986. Ontogenic development of T and B cells and non-lymphoid cells in the white pulp of human spleen. Immunology **57:**61–69.

35. **Ochsenbein, A. F., and R. M. Zinkernagel.** 2000. Natural antibodies and complement link innate and acquired immunity. Immunol. Today **21:**624–630.

36. **Prescott, S. L., C. Macaubas, B. J. Holt, T. B. Smallacombe, R. Loh, P. D. Sly, and P. G. Holt.** 1998. Transplacental priming of the human immune system to environmental allergens: universal skewing of initial T cell responses toward the Th2 cytokine profile. J. Immunol. **160:**4730–4737.

37. **Reimann, K. A., B. C. Waite, D. E. Lee-Parritz, W. Lin, B. Uchanska-Ziegler, M. J. O'Connell, and N. L. Letvin.** 1994. Use of human leukocyte-specific monoclonal antibodies for clinically immunophenotyping lymphocytes of rhesus monkeys. Cytometry **17:**102–108.

38. **Ridge, J. P., E. J. Fuchs, and P. Matzinger.** 1996. Neonatal tolerance revisited: turning on newborn T cells with dendritic cells. Science **271:**1723–1726.

39. **Solvason, N., A. Lehuen, and J. F. Kearney.** 1991. An embryonic source of Ly1 but not conventional B cells. Int. Immunol. **3:**543–550.

40. **Sopper, S., C. Stahl-Hennig, M. Demuth, I. C. Johnston, R. Dorries, and V. ter Meulen.** 1997. Lymphocyte subsets and expression of differentiation markers in blood and lymphoid organs of rhesus monkeys. Cytometry **29:**351–362.

41. **Spencer, J., P. G. Isaacson, J. A. Walker-Smith, and T. T. MacDonald.** 1989. Heterogeneity in intraepithelial lymphocyte subpopulations in fetal and postnatal human small intestine. J. Pediatr. Gastroenterol. Nutr. **9:**173–177.

42. **Spencer, J., T. T. MacDonald, T. Finn, and P. G. Isaacson.** 1986. The development of gut associated lymphoid tissue in the terminal ileum of fetal human intestine. Clin. Exp. Immunol. **64:**536–543.

43. **Stall, A. M., S. M. Wells, and K. P. Lam.** 1996. B-1 cells: unique origins and functions. Semin. Immunol. **8:**45–59.

44. **Tarantal, A. F., and M. J. Cowan.** 1999. Administration of recombinant human stem cell factor (rhSCF) and granulocyte-colony stimulating factor (rhG-CSF) to maternal and fetal rhesus monkeys (Macaca mulatta). Cytokine **11:**290–300.

45. **Tarantal, A. F., O. Goldstein, F. Barley, and M. J. Cowan.** 2000. Transplantation of human peripheral blood stem cells into fetal rhesus monkeys (Macaca mulatta). Transplantation **69:**1818–1823.

46. **Tarantal, A. F., and A. G. Hendrickx.** 1988. Use of ultrasound for early pregnancy detection in the rhesus and cynomolgus macaque (Macaca mulatta and Macaca fascicularis). J. Med. Primatol. **17:**105–112.

47. **Tarantal, A. F., M. L. Marthas, S. E. Gargosky, M. Otsyula, M. B. McChesney, C. J. Miller, and A. G. Hendrickx.** 1995. Effects of viral virulence on intrauterine growth in SIV-infected fetal rhesus macaques (Macaca mulatta). J. Acquir. Immune. Defic. Syndr. Hum. Retrovirol. **10:**129–138.

48. **Toivanen, P., J. Uksila, A. Leino, O. Lassila, T. Hirvonen, and O. Ruuskanen.** 1981. Development of mitogen responding T cells and natural killer cells in the human fetus. Immunol. Rev. **57:**89–105.

49. **Watts, A. M., J. R. Stanley, M. H. Shearer, P. S. Hefty, and R. C. Kennedy.** 1999. Fetal immunization of baboons induces a fetal-specific antibody response. Nat. Med. **5:**427–430.

50. **Wilson, C., D. Lewis, and L. Penix.** 1996. The physiologic immunodeficiency of immaturity, p. 253–295. *In* E. Stiehm (ed.), Immunologic disorders in infants and children, 4th ed. The W. B. Saunders Co., Philadelphia, PA.

51. **Youinou, P., C. Jamin, and P. M. Lydyard.** 1999. CD5 expression in human B-cell populations. Immunol. Today **20:**312–316.